Optical hole burning and spectral diffusion in ruby

A. Szabo and R. Kaarli*
Institute of Microstructural Sciences, National Research Council of Canada, Ottawa, Ontario, Canada K1A 0R6
(Received 1 July 1991)

Frequency-domain optical hole burning of the R_1 line [$^4A_2(-\frac{1}{2}) \leftrightarrow \bar{E}(-\frac{1}{2})$ transition] in dilute ruby is studied at 2 K and with a field of 3.6 kG applied along the c axis. A pump-probe (PP) technique is used with precise probe-frequency shifting obtained by an acousto-optic modulator. For sufficiently short PP pulses (50 μs), two holes (narrow and wide) are observed. The narrow ($\sim$20 kHz half width at half maximum at low power) hole-width dependence on Rabi frequency approximately agrees with that inferred from free-induction-decay measurements. For the present concentration (0.0034 wt. % Cr_2O_3) and field, the narrow hole width is determined by fluctuating fields produced by Cr-Cr spin flips [A. Szabo, T. Muramoto, and R. Kaarli, Phys. Rev. B **42**, 7769 (1990)]. When the PP delay time is varied, the amplitude of the narrow hole decays with a $1/e$ time constant of $\sim$300 μs compared to the $\bar{E}$ fluorescence lifetime of 4 ms. The wide hole ($\sim$500 kHz half width at half maximum) is due to Al-Cr superhyperfine interactions and is created by a spectral diffusion mechanism driven by Al-spin flipping in the host lattice.

I. INTRODUCTION

Following the initial experimental demonstration by Brewer and DeVoe[1] of the failure of the optical Bloch equations (OBE) in describing the saturation of an optical transition in a solid ($Pr:LaF_3$), a large number of theoretical[2–10] studies have appeared as well as further experimental work[11–13] (in ruby, $Cr:Al_2O_3$). As discussed by Berman,[7] quantitative understanding of the saturation behavior has not yet been achieved and further experimental studies are needed. In particular, Yamanoi and Eberly[3] have suggested frequency-domain [hole-burning (HB)] studies to further test the various theories. As discussed earlier,[14] HB can provide useful additional tests since, for the finite preparation times employed in the experiments, the various theories predict differing complicated hole shapes in contrast to time-domain [free-induction-decay (FID)] predictions that look similar in shape for the various theories.

Our first measurements[13] of high-resolution HB of the R_1 line in ruby showed that HB widths were $\sim$10 times larger than the FID widths. The purpose of this paper is to explain this discrepancy and to outline conditions under which agreement between HB and FID widths is obtained. The underlying cause of this effect is shown to be spectral diffusion.

II. EXPERIMENT

A. Hole burning

The setup used for the HB studies is shown in Fig. 1. The $^4A_2(-\frac{1}{2}) \leftrightarrow \bar{E}(-\frac{1}{2})$ transition (selected by a circular polarizer) in 0.0034-wt % Cr_2O_3 dilute ruby was studied. As in earlier work,[11–13] a field of 3.6 kG was applied along the c axis and the sample temperature was 2 K. A Coherent model 699-21 dye laser was modified[12] to give a peak-to-peak laser linewidth <2 kHz for times of $\sim$1 ms. A pump-probe sequence of laser pulses,[13,15] repeated at 25 Hz, was used to measure the hole shape. Except where noted, all data was obtained for a pump (=probe) width of 50 μs with a 10-μs pump-probe separation time. The probe power was typically 1–5 % of the pump power. The light pulses were gated out of the cw beam by an acousto-optic modulator (AOM) driven successively by a fixed-frequency stable oscillator for the pump and a computer-controlled frequency synthesizer to provide scanning probe rf pulses. The pump and probe pulse widths were equal and the boxcar gate was one-half the pulse width and set on the last half of the probe pulse. Following the AOM, the beam was split into "sample" and "reference" beams which were detected by silicon photodiodes with a common 600 Ω load and the signals subtracted to reduce amplitude noise and prevent over-

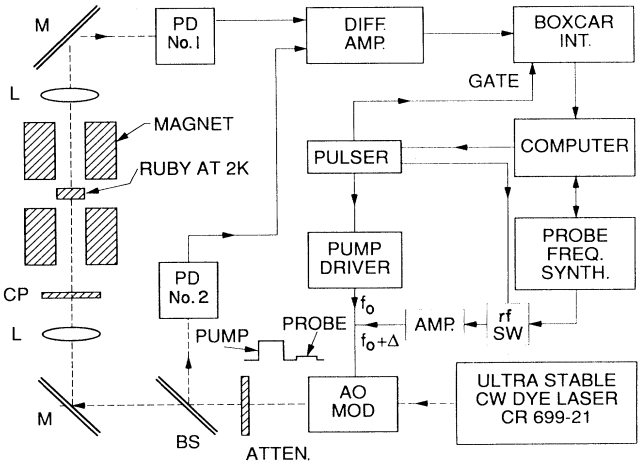

FIG. 1. Experimental setup for pump-probe hole-burning studies (see text).

loading of the amplifier by the pump pulse. (Not shown in Fig. 1 are AOM switches in front of the two diodes to further suppress the pump pulse signals.) Following subtraction, the probe signal was amplified by a low-noise amplifier (Stanford model SR560) and averaged by a boxcar integrator. Each run consisted of 101 points taken at 3-s intervals. The entire experiment was under computer control with the data and experimental parameters stored on magnetic disc for later analysis.

B. Free-induction decay

The FID signal was directly detected by a photodiode using an AOM to suppress the preparation optical pulse. While not quite as sensitive as the heterodyne scheme used earlier,[12] it was not susceptible to the technical noise problems of the heterodyne method resulting in less scatter of the data. Also, since no local oscillator beam exists in the sample, disturbance[1,16] of the induced coherence cannot occur. The diode signal was amplified by either a low-noise, high-gain amplifier of 1-MHz bandwidth (Stanford model SR560) or a 10-MHz bandwidth amplifier (Evans model 4163) for the faster decay times (<1.5 μs) at higher Rabi frequencies. The decay signals were then averaged by a Data Precision 6100 digital oscilloscope with a model 660B plug in.

C. Rabi frequency measurements

The Rabi frequency was measured by observation of the nutation frequency at high powers. The value obtained is, of course, some average over the Gaussian beam shape. As shown by Shoemaker and Stryland,[17] however, beam profile effects do not significantly affect the nutation frequency. Typically the observed nutation frequency is within 10% of that calculated using the field intensity of the center of the beam.

III. RESULTS

A. Free-induction decay

Examples of FID data are summarized in Fig. 2. The hole half-width, W_F, derived from the FID decays is calculated from the equation

$$W_F=(1/2\pi)[1/(2T_{\rm obs})-1/T_2]\ , \tag{1}$$

where $T_{\rm obs}$ is the observed decay time and T_2 is the dephasing time measured by photon echoes. (For the present ruby, $T_2=15$ μs.) $T_{\rm obs}$ is obtained by a regression analysis fit to ~ 2 orders of FID intensity decay. It should be noted from Fig. 2 that the FID decay is not a single exponential, thus the values $T_{\rm obs}$ represent an average decay. In particular, for large Rabi frequencies, there is a fast initial decay followed by a slow decay. The regression analysis emphasizes the slow decay and this should be borne in mind for the derived hole widths presented later. For example, the hole width obtained from the initial part of the decay ($f_R=172$ kHz) in Fig. 2 gives $W_F=83$ kHz compared to $W_F=58$ kHz obtained by averaging over the entire decay. Finally, for small

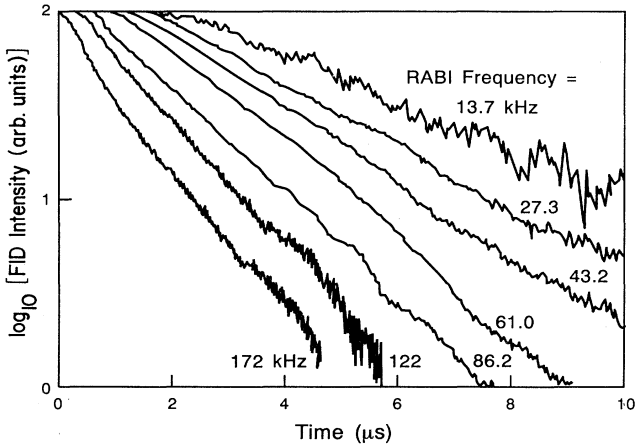

FIG. 2. Summary of free-induction decays observed for a range of Rabi frequencies.

Rabi frequencies, we found that $T_{\rm obs}\rightarrow T_2/4$ giving $W_F=1/(2\pi T_2)$, the normal optical Bloch result for the linewidth of the population term w of the Bloch vector (u,v,w).

B. Hole burning

Examples of the HB data are shown in Fig. 3 along with a regression analysis fit to a Lorentzian line shape. Figure 4 shows HB data over a wider frequency range. This plot illustrates that the narrow central hole (Fig. 3) sits on a wide hole. The amplitude of the wide hole relative to the narrow hole is found to increase as, (1) the length of the pump pulse increases, (2) the separation between the pump-probe pulses increases, and (3) the Rabi frequency increases.

An example of (1) is shown in Fig. 5 taken from earlier reported data[13] for a pump and probe pulse of 300 μs separated by 100 μs. Under these conditions, only the wide hole is seen. For an intermediate pumping time of 100 μs, Fig. 6 shows a case where the broad and narrow holes have about equal amplitude. Earlier studies[15] of the hole dependence on pump-probe separation show that, for a separation time $\gtrsim 300$ μs, the narrow hole disappears and only the broad hole remains.

C. Summary of data

The dependence of the hole widths derived from the FID and HB data (narrow hole) on the Rabi frequency is shown in Fig. 7. For Rabi frequencies $\gtrsim 100$ kHz, no HB data is plotted since it becomes difficult to separate the narrow and wide holes. If $W_{\rm obs}$ is the observed half-width of the hole, the deconvoluted width W_H (plotted in Fig. 7) is given by

$$W_H=W_{\rm obs}-1/(2\pi T_2)\ , \tag{2}$$

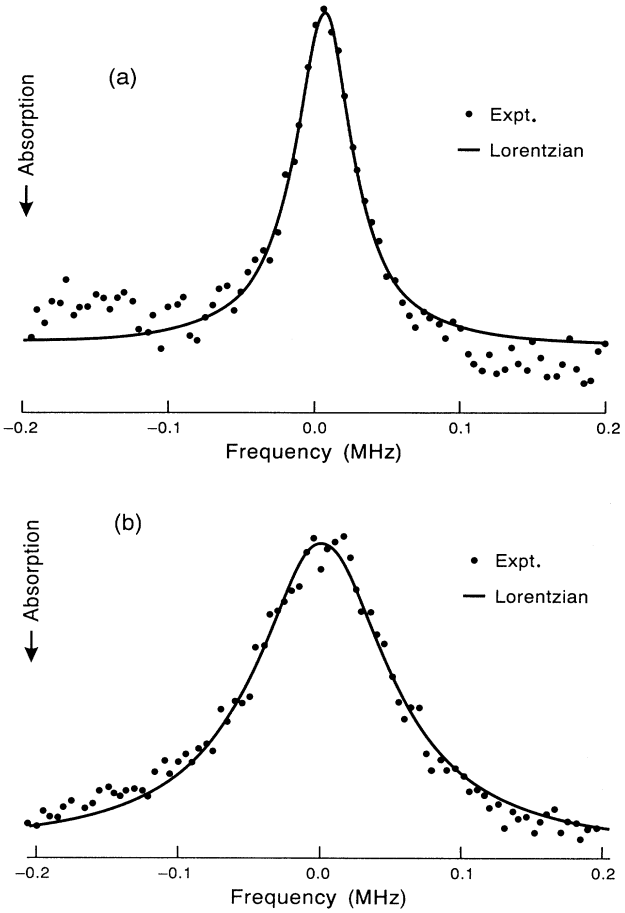

FIG. 3. Examples of hole shapes seen for Rabi frequencies (a) 8.9 kHz and (b) 70 kHz. The solid curves show a regression analysis fit of a Lorentzian shape to the data. Pump and probe pulsewidths = 50 μs.

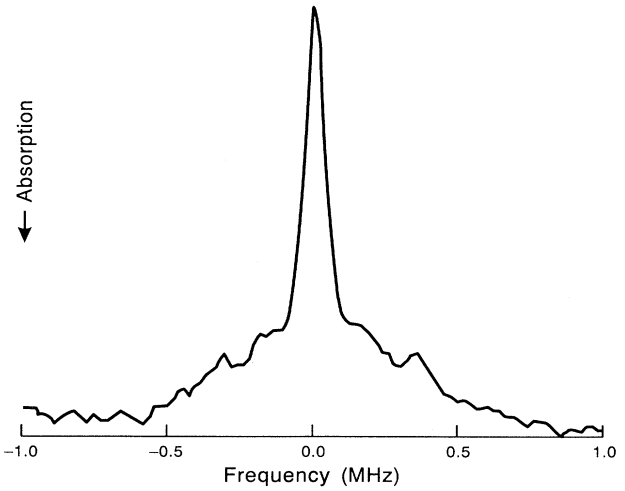

FIG. 4. Example of hole shape observed over a wider frequency range than in Fig. 3. A narrow hole is observed sitting on a wide hole. Rabi frequency = 36 kHz and pump and probe pulsewidths = 50 μs.

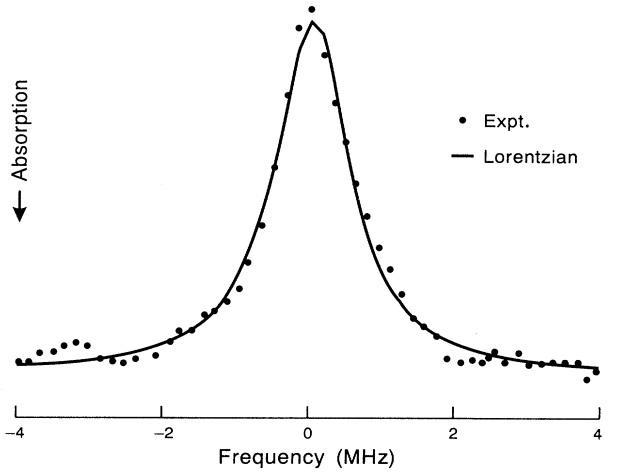

FIG. 5. Hole shape observed when the pump and probe pulsewidths are increased to 300 μs. Rabi frequency = 105 kHz.

where we subtract the homogeneous width associated with the probe from the observed width. Not included in Eq. (2) is the width arising from the finite width of the probe pulse. This is difficult to include precisely since the line shape from this source is not Lorentzian. Numerical calculations show, however, that the correction to the width is small; ~3 kHz for a 50-μs pulse. This was estimated from the difference between the calculated hole width at a low Rabi frequency (1 kHz) for cw excitation [$1/(2\pi T_2)=10.6$ kHz] and for 50-μs pulses (~16 kHz), using the standard Bloch equations.[14]

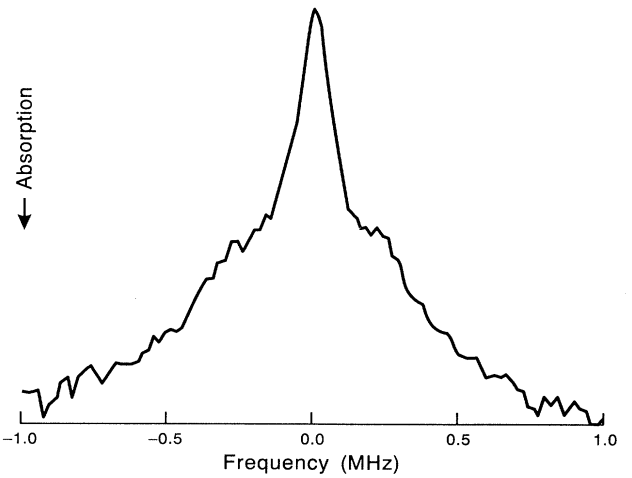

FIG. 6. Hole shape showing an increase in the amplitude of the wide hole relative to the narrow hole as the laser intensity is increased. Compare to Fig. 4, Rabi frequency = 90 kHz and pump pulsewidth = 100 μs and probe width = 50 μs.

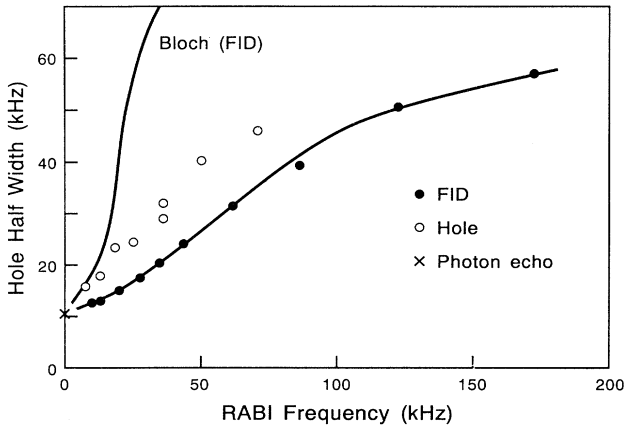

FIG. 7. Rabi frequency dependence of hole widths obtained from time-domain (free-induction decay) and frequency-domain (hole-burning) measurements.

IV. DISCUSSION

A. Comparison of frequency- and time-domain linewidths

A central result of this study is that near agreement is now observed between frequency- and time-domain derived linewidths (Fig. 7) using short (50-μs) pump-probe pulses. Earlier studies[13] using 300-μs pump-probe pulses gave frequency-domain widths about an order of magnitude larger than that inferred from time-domain (FID) data.

An intuitive explanation for the frequency-domain results might be that the hole width depends on fluence as shown by earlier calculations[18] using the standard OBE. Table I shows hole widths calculated using the standard OBE and two popular models for the modified OBE, (1) Gauss-Markov[6] and (2) random telegraph.[5] The modified OBE predict widths that are almost independent of preparation pulse lengths between 50 and 300 μs, unlike the standard OBE. Although the modified OBE are certainly not "correct" in explaining all features of optical saturation (in particular, hole shapes as will be discussed later), they appear to approximately describe[12] the FID behavior, unlike the standard OBE which fail badly. We conclude that the increasing hole width as the preparation time is increased is not a fluence effect.

TABLE I. Comparison of theoretical and experimental hole half-width dependence on the width of the preparation pulse. In the calculation we assume the parameters, $T_1=4200$ μs, $T_2=15$ μs, correlation time $=15$ μs, and a Rabi frequency $=100$ kHz. Also, the nutation structure (e.g., Fig. 8) is averaged out in calculating the width.

	Hole half-width (kHz)			
Preparation time (μs)	Optical Bloch	Gauss-Markov	Random telegraph	Expt.
50	240	96	101	~60
300	530	104	104	610
cw	1673	147	130	

B. Hole shapes

Figure 3 shows that the experimental hole shapes are Lorenztian consistent with the observed exponential decay of the FID (for Rabi frequencies <100 kHz). These hole shapes disagree sharply with those predicted by the standard or modified OBE. Theoretical hole shapes are shown in Fig. 8 for a Rabi frequency $=70$ kHz and a preparation time of 50 μs (pulse angle$=7\pi$). Generally all theories predict nutation structure in the hole. In particular, as discussed earlier,[14] the Gauss-Markov model gives a long effective dephasing time near the center of the line and hence shows much deeper fluctuations there. As the pulse angle varies over multiples of π, the Bloch vector component w at the center of the hole varies approximately between $+1$ and -1 for the Gauss-Markov model. Experimentally, such a variation is not seen and the signal at the center of the line is always absorptive. To some extent, the observed hole shape will be smoothed out by two factors: (1) convolution of the homogeneous line shape (10.6-kHz half-width) with w, and (2) the effect of a Gaussian beam shape. These points remain to be studied in detail. However, the main factor in determining the hole shape is, we believe, spectral diffusion during the pump-probe sequence.

C. Spectral diffusion

Earlier work here[15] (in which the pump-probe separation was varied), as well as the power and pump time dependence of the relative amplitudes of the narrow and wide holes in the present work, suggests that the transfer of excitation between the two holes is due to *spectral*

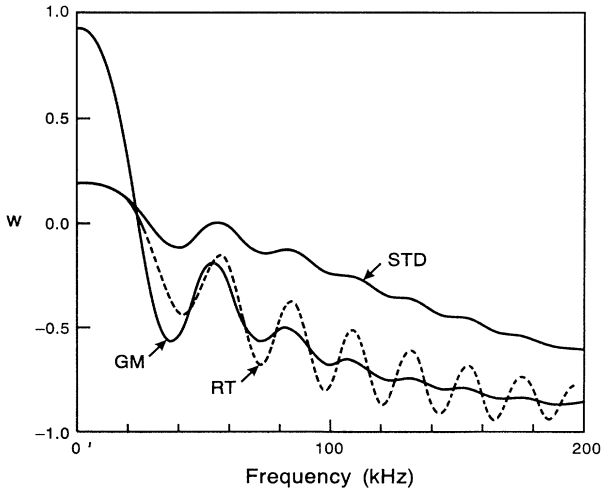

FIG. 8. Theoretical hole shapes for a Rabi frequency $=70$ kHz [compare to Fig. 3(b)], and three models for the optical Bloch equations: (1) standard (STD), (2) Gauss-Markov (GM), and (3) random telegraph (RT).

diffusion (SD). Before discussing the mechanisms for this in detail, we first briefly review SD concepts evolved for magnetic resonance and discuss some additional concepts needed to describe SD for optical transitions.

1. Background

The concept of spectral diffusion was first introduced in studies of magnetic resonance spectra. As noted by Klauder and Anderson[19] in 1962, SD is "an immensely complicated question." Thirty years later, the complications, both conceptual and experimental, still remain. The current description of SD rests on the recognition of at least three kinds of line broadening and the idea of spin or resonance "packets."[19–22] The most common types of broadening in solids, inhomogeneous and homogeneous, are well defined and understood. The former arises from static variations in ion frequencies due to various host defects and is observed in conventional linear spectroscopy. An operational definition of the homogeneous linewidth is that it equals $1/(\pi T_2)$ (FWHM), where T_2 is the dephasing time measured by echoes (assuming it has a Lorentzian shape), or, in general, is given by the Fourier transform of the echo decay. In solids, at sufficiently low temperatures and for which $T_2 \ll T_1$, the dephasing source is thought to be ultimately due to flip-flops of the host and dopant spins. The spin flips produce magnetic fluctuations and hence corresponding frequency jitter of the ion under study. While it is obvious that hole burning will occur for homogeneously broadened lines distributed over a larger inhomogeneous width, it is not clear what will happen in the presence of a third type of broadening called quasistatic or heterogeneous.[23,24] Such broadening results from all possible configurations of host spin orientations around a given ion. It can be thought of as a time-dependent inhomogeneous broadening. In the packet description of saturation, we imagine that ions within a homogeneous linewidth from the excitation frequency will be excited and that this excitation will be carried over the heterogeneous linewidth as the spin orientations evolve. A spectral diffusion time T_d can be defined as the time in which the frequency of an ion remains within a homogeneous width.

In magnetic resonance, T_d has been indirectly obtained from saturation measurements,[22,25] however as far as the authors are aware, no frequency-domain observations has been made of hole burning of a heterogeneously broadened line. To give a feel for the various widths and lifetimes for Cr^{3+} magnetic resonance in the ruby ground state, a value of $T_d = 14$ μs has been inferred[25] using a transient saturation technique and $T_2 \sim 4$ μs (homogeneous width $=0.08$ MHz) measured by echoes.[26,27] This is for a sample of $\sim 0.005\%$ concentration at fields 4–6 kG along the c axis. The heterogeneous width due to Cr-Al superhyperfine (shf) broadening is ~ 35 MHz.[28] In summary, while the fluctuating packet description of saturation (as has evolved from the Portis[20] original static model) is appealing from a conceptual and theoretical view, some caution is needed in adopting this picture as has been emphasized by Klauder and Anderson.[19] In the case of optical transitions, SD assumes other complexities as will now be discussed.

If SD is operationally defined as any process that produces a change in the inhomogeneously broadened absorption line outside a monochromatically excited homogeneous packet, then there are at least three distinct processes that produce SD. (1) Energy transfer (spatial transport): (a) spin-spin cross relaxation (direct process) and (b) phonon-assisted transfer. (2) Environmental changes (no spatial transport): (a) host and impurity spin flipping (indirect process), (b) instantaneous diffusion, (c) lattice changes (two-level systems), and (d) optically induced dynamic nuclear polarization. (3) Optical pumping.

We now briefly discuss some examples of these processes. 1(a) has been observed[29] in cw optical hole-burning experiments in ruby that showed a decrease of the entire R_1 inhomogeneous absorption line as well as a hole when the ${}^4A_2(\pm\frac{1}{2}) \rightarrow \bar{E}(\pm\frac{1}{2})$ line of Cr^{3+} was pumped with a single-frequency laser. This result was shown to arise from Cr-Cr electron spin flipping in the ground state between ions resonant with the laser and nonresonant ions. We note that, using the terminology of Mims,[30] this is a *direct* spin process as opposed to 2(a) which is an *indirect* spin process. Process 1(b) has been observed[21] in concentrated ruby and other materials at temperatures > 10 K. The overall effect of phonon-induced diffusion is the same as 1(a) in that the entire inhomogeneous line is affected by narrowband pumping.

Process 2(a) is the one discussed earlier to explain SD in magnetic resonance. It has also been used[32] to describe optical SD (Ref. 33) in the system Pr^{3+}:CaF_3. Unlike process 1, this process produces SD over a frequency region determined by the spin-spin and/or exchange interaction strength. The width of the SD is typically in the range 0.1–10 MHz depending on whether nuclear or electronic spins are involved. An example is the heterogeneous dipolar broadened optical line width of ~ 80 kHz of the ${}^3H_4 \leftrightarrow {}^1D_2$ transition of Pr^{3+} in LaF_3 (homogeneous width ~ 20 kHz) produced by Pr-F nuclear spin dipolar interactions.[34]

Instantaneous diffusion[30] [2(b)] has recently been observed in the optical region[35] and arises because of the frequency shift produced by nearby excited ions via an electric dipole interaction. The observed shifts were in the range 10–100 kHz for the system Eu^{3+}:Y_2O_3. Process 2(c) is usually seen[36,37] in glasses and is much slower ($T_d \sim$ s) than diffusion times in crystals. Processes 2(d) and 3 may be related, however, the mechanism of optically induced nuclear polarization in solids is poorly understood.[38] Evidently, 2(d) is an intensity-dependent effect and results in nuclear ordering as suggested earlier by DeVoe and Brewer.[1] Finally, an example of 3 is the hole width seen[33] at long times following optical excitation in the ${}^3H_4 \rightarrow {}^1D_2$ transition of Pr^{3+} in CaF_2. A width of 9 MHz is measured compared to the homogeneous width of 0.37 MHz observed by echoes or delayed free-induction decay. It appears that spectral diffusion in this material involves a complex series of processes starting with indirect spin-flipping-induced diffusion outside the frozen cores at short times, followed by optical pumping

of the ground-state levels at times corresponding to the fluorescence lifetime (500 μs) and finally spin flipping in the frozen core at longer times (s).

2. *Spectral diffusion in ruby*

We believe that indirect spin flipping [process 2(a)] is responsible for optical SD in ruby. In ruby there are four spin systems to consider: (1) the Cr electronic spins in resonance and (2) nonresonant with the laser, (3) Al nuclear spins in the frozen core, and (4) Al spins just outside the core (i.e., bulk spins). In addition, there are three optical linewidths to consider as discussed earlier. For the dilute ruby used here, these linewidths have the FWHM values: inhomogeneous[39] $\sim$2 GHz, heterogeneous[40] $=1.2$ MHz, and homogeneous[41] $\sim$20 kHz. We note that, if the crystal were perfect, then linear spectroscopy would display the heterogeneous width. The homogeneous width, in principle, could be seen if a single ion could be observed assuming (a) the measurement was made in a time short compared to changes in the surrounding Al nuclear orientations and (b) the Cr-Al complex was initially prepared to be in the same state. In practice, (b) would be nearly impossible to achieve (there are 6^{13} possible Al configurations in the first shell surrounding a Cr ion) which, along with optical pumping, would cause the optical absorption to jump around making direct frequency-domain observation of the homogeneous width difficult.

We identify the wide hole ($\sim$1 MHz FWHM) in Figs. 4 and 6 as heterogeneous and the narrow hole as homogeneous. The heterogeneous width is due to the Cr-Al shf interaction, whereas the homogeneous width still seems to be controlled by Cr-Cr interactions,[38] even for the present very dilute ruby. The increasing amplitude of the wide hole relative to the narrow hole as the laser intensity is increased is consistent with a packet model of SD in which the optical frequency of a given ion drifts in and out of resonance with the laser. The rate of this drift was measured by fixing the probe frequency equal to the pump frequency and observing the decay of the narrow line as the pump-probe spacing was varied (Fig. 9). This measurement shows that the narrow line completely collapses into the broad line with a $1/e$ time of $\sim$300 μs. This time does not correspond to any of the known relaxation processes in ruby as summarized in Table II. We note that processes 1(a) and 2(a) both can contribute to the narrow line decay. However, the Cr-Cr direct spin-flip process of 1(a) is too slow (2500-μs time constant[38]) to account for the observed 300-μs decay.

To answer the question if indirect Cr-Cr flips can produce SD over the $\sim$1-MHz wide line, we estimate the Cr-Cr dipolar broadened width of the R_1 optical transition. First consider the static dipolar broadening, $\Delta_{\rm dip}$ (FWHM) in the ground state. For $S=\frac{3}{2}$, we have approximately[42]

$$\Delta_{\rm dip}=10(gB)^2n/h \ .$$

For 0.0034% ruby, $n=1.08\times10^{18}$ ions/cm^3 giving $\Delta_{\rm dip}=560$ kHz. For the optical transition,[42] the effective magnetic gyromagnetic ratio is reduced from the ground-state value by the factor $(g_{\rm ex}-g_{\rm gr})/(2g_{\rm gr})=0.12$, where $g_{\rm ex}$ ($g_{\rm gr}$) are excited (ground-state) g values. This gives an optical dipolar width of 0.07 MHz $\ll$ observed heterogeneous width. We conclude that Cr spin flipping cannot explain the SD that leads to the narrow line decay.

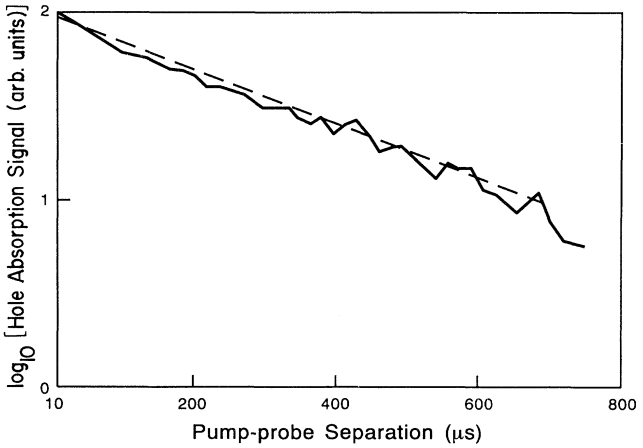

FIG. 9. Decay of the peak of the narrow hole following a 50-μs preparation pulse. Rabi frequency $=8.6$ kHz. The dashed line is a regression analysis fit to the decay.

This leaves only the Cr-Al shf interactions which are further supported by the good agreement between Endo's[40] calculated heterogeneous width of 1.2 MHz versus the observed value of 0.8–1.2 MHz (Figs. 4–6). It is not clear if SD is due to flip-flops in the Al frozen core by, e.g., the mechanism suggested by Shakhmurotov[43] or by Al spin flipping in the bulk lattice. However, the fact that the narrow hole collapses into the wide one without appreciable broadening of the line suggests that the frequency jumps are $\gg$ homogeneous width pointing to the frozen core.

TABLE II. A summary of various relaxation times in dilute (0.0034 Cr_2O_3 wt %) ruby at 2 K and with a magnetic field of $\sim$4 kG along the crystal axis.

Cr relaxation process	Decay time (μs)
$\bar{E}$ fluorescence	4200
$^4A_2$ spin lattice	5×10^5
Optical (R_1) dephasing[a]	15
Electron spin ($^4A_2$) dephasing[b]	7
Resonant electron spin flip[a]	2500
Al relaxation process	
Spin lattice	$>6\times10^7$
Bulk dephasing[c]	50
Frozen-core dephasing[a]	1200

[a]Reference 38.
[b]References 26 and 27.
[c]Reference 25.

A similar conclusion was reached by Boscaino *et al.*[25] in their SD studies of electron spin resonance of Cr^{3+} in ruby. Also, recent photon-echo studies[44] point to the role of frozen-core dynamics in explaining in nonexponential echo decay. Modeling of the various processes that produce optical dephasing and spectral diffusion is presently in progress.[45]

V. CONCLUSIONS

Our optical hole-burning studies in ruby show the preparation time is an important consideration in determining the observed hole width. This time, together with the observation time, must be less than the spectral diffusion time if correspondence is to be achieved between frequency- and time-domain derived hole widths. The observed spectral diffusion time of ~ 300 μs over a width of ~ 1 MHz is mainly determined by Al-nuclear-spin flips in the host lattice, probably in the frozen core.

ACKNOWLEDGMENTS

One of us (A.S.) thanks R. N. Shakhmuratov for many interesting discussions. We thank J. Froemel for his excellent technical assistance.

*Present address: Institute of Physics, Tartu, Estonia.

[1]R. G. DeVoe and R. G. Brewer, Phys. Rev. Lett. **50**, 1269 (1983).
[2]E. Hanamura, J. Phys. Soc. Jpn. **52**, 3678 (1983).
[3]M. Yamanoi and J. H. Eberly, J. Opt. Soc. Am. B **1**, 751 (1984).
[4]J. Javanainen, Opt. Commun. **50**, 26 (1984).
[5]K. Wodkiewicz and J. H. Eberly, Phys. Rev. A **32**, 992 (1985).
[6]P. R. Berman and R. G. Brewer, Phys. Rev. A **32**, 2784 (1985).
[7]P. R. Berman, J. Opt. Soc. Am. B **3**, 564 (1986); **3**, 572 (1986).
[8]A. R. Kessel, R. N. Shakhmuratov, and L. D. Eskin, Zh. Eksp. Teor. Fiz. **94**, 202 (1988) [Sov. Phys. JETP **67**, 2071 (1988)].
[9]P. A. Apanasevich, S. Ya. Kilin, and A. P. Nizovtsev, J. Appl. Spectrosc. **47**, 1213 (1988).
[10]A. I. Burshtein, A. A. Zharikov, and V. A. Malinovskii, Zh. Eksp. Teor. Fiz. **96**, 2061 (1989) [Sov. Phys. JETP **69**, 1164 (1989)].
[11]T. Muramoto and A. Szabo, Phys. Rev. A **38**, 5928 (1988).
[12]A. Szabo and T. Muramoto, Phys. Rev. A **39**, 3992 (1989).
[13]A. Szabo, T. Muramoto, and R. Kaarli, in *Coherence and Quantum Optics VI,* edited by J. H. Eberly, L. Mandel, and E. Wolf (Plenum, New York, 1990), pp. 1131–1135.
[14]A. Szabo and T. Muramoto, Phys. Rev. A **37**, 4040 (1988).
[15]A. Szabo, in *Proceedings of the Tenth Vavilov Conference on Nonlinear Optics* (NOVA Science Publishers, New York, in press).
[16]R. M. MacFarlane, R. M. Shelby, and R. L. Shoemaker, Phys. Rev. Lett. **43**, 1726 (1979).
[17]R. L. Shoemaker and E. W. Stryland, J. Chem. Phys. **64**, 1733 (1976).
[18]T. Endo, T. Muramoto, and T. Hashi, Opt. Commun. **45**, 122 (1983).
[19]J. R. Klauder and P. W. Anderson, Phys. Rev. **125**, 912 (1962).
[20]A. M. Portis, Phys. Rev. **91**, 1070 (1953).
[21]T. G. Castner, Phys. Rev. **115**, 1506 (1959).
[22]S. Clough and C. A. Scott, J. Phys. C **1**, 919 (1968).
[23]M. Mehring, *Principles of High Resolution NMR in Solids* (Springer-Verlag, Berlin, 1983), p. 304.
[24]R. Kubo, in *Fluctuation, Relaxation and Resonance in Magnetic Systems,* edited by P. Ter Haar (Oliver and Boyd, London, 1962), p. 23.
[25]R. Boscaino, F. M. Gelardi, and R. M. Mantegna, in *Structure and Dynamics of Molecular Systems,* edited by R. Daudel *et al.* (Reidel, Dordrecht, 1985), p. 149.
[26]P. F. Liao and S. R. Hartmann, Opt. Commun. **8**, 310 (1973).
[27]D. R. Taylor and J. P. Hessler, Phys. Lett. **53A**, 451 (1975).
[28]R. F. Wenzel, Phys. Rev. B **1**, 3109 (1970).
[29]P. E. Jessop and A. Szabo, in *Proceedings of the Fifth International Conference on Laser Spectroscopy,* edited by A. R. W. McKellar, T. Oka, and B. P. Stoicheff (Springer-Verlag, Berlin, 1981), pp. 408–411.
[30]W. B. Mims, in *Electron Paramagnetic Resonance,* edited by S. Geschwind (Plenum, New York, 1972), pp. 263–351.
[31]P. M. Selzer, D. S. Hamilton, and W. M. Yen, Phys. Rev. Lett. **38**, 858 (1977).
[32]Y. S. Bai and M. D. Fayer, Phys. Rev. B **39**, 11 066 (1989).
[33]R. M. Shelby and R. M. MacFarlane, J. Lumin. **31&32**, 839 (1984).
[34]R. G. DeVoe, A. Wokaun, S. C. Rand, and R. G. Brewer, Phys. Rev. B **23**, 3125 (1981).
[35]J. Huang, J. M. Zhang, A. Lezama, and T. W. Mossberg, Phys. Rev. Lett. **63**, 78 (1989).
[36]W. Breinl, J. Friedrich, and D. Haarer, J. Chem. Phys. **81**, 3915 (1984).
[37]K. A. Littau, Y. S. Bai, and M. D. Fayer, J. Chem. Phys. **92**, 4145 (1990).
[38]A. Szabo, T. Muramoto, and R. Kaarli, Phys. Rev. B **42**, 7769 (1990).
[39]A. Szabo, Opt. Commun. **33**, 301 (1980).
[40]T. Endo, T. Muramoto, and T. Hashi, Phys. Lett. **99A**, 128 (1983).
[41]A. Szabo, J. Opt. Soc. Am. **3**, 514 (1986).
[42]As discussed in A. Compaan, Phys. Rev. B **5**, 4450 (1972), we take the quasistatic width to be $\frac{2}{3}$ the total dipolar width.
[43]R. N. Shakhmuratov, Pis'ma Zh. Eksp. Teor. Fiz. **51**, 454 (1990) [JETP Lett. **51**, 513 (1990)].
[44]J. Ganem, Y. P. Wang, D. Boye, R. S. Meltzer, W. M. Yen, R. Wannemacher, and R. M. MacFarlane, Phys. Rev. Lett. **66**, 695 (1991); J. Ganem, Y. P. Wang, R. S. Meltzer, and W. M. Yen, Phys. Rev. B **43**, 8599 (1991).
[45]R. N. Shakmuratov and A. Szabo (unpublished).